

THE KINETICS AND THE MECHANISM OF OZONE PHOTOLYSIS AT 253.7 nm

C. COBOS, E. CASTELLANO and H. J. SCHUMACHER

Instituto de Investigaciones Fisicoquímicas Teóricas y Aplicadas, Sucursal 4, Casilla de Correo 16, 1900 La Plata (Argentina)

(Received August 18, 1982)

Summary

The photolysis of ozone by steady illumination at 253.7 nm and 25 °C was studied using two different techniques. In one the ozone decomposition from an initial pressure of 50 Torr was measured manometrically at constant volume and in the other the decomposition from an initial pressure of 1 - 2 Torr was measured photometrically by monitoring changes in the optical absorption. In both cases the light intensity was measured during each irradiation period. The experiments were performed in pure ozone and in ozone containing oxygen, helium, sulphur hexafluoride and nitrogen.

The quantum yield Φ of the decomposition of pure ozone was 5.68 ± 0.15 molecules quantum⁻¹ and was pressure independent. The quantum yields Φ_{He} and Φ_{SF_6} of the decomposition of ozone in He-O₃ ($p_{\text{He}}/p_{\text{O}_3} \approx 600$) and SF₆-O₃ ($p_{\text{SF}_6}/p_{\text{O}_3} \approx 300$) were 5.62 ± 0.41 molecules quantum⁻¹ and 5.44 ± 0.32 molecules quantum⁻¹ respectively. In N₂-O₃ mixtures with high values of $p_{\text{N}_2}/p_{\text{O}_3}$, the quantum yield decreases to 4 molecules quantum⁻¹. Oxygen has a strong inhibiting effect. All the experimental data can be quantitatively explained using the following mechanism:





The quantum yield ϕ for $\text{O}(^1\text{D})$ production is 0.92 ± 0.04 atoms quantum⁻¹. The unspecified O_2^* molecule is formed with an efficiency of 0.47 ± 0.15 . Under our experimental conditions O_2^* molecules are highly resistant to collisional deactivation and most are removed via reaction (4a). The efficiency of deactivation of $\text{O}(^1\text{D})$ atoms by N_2 is 0.19 ± 0.01 . A value of 0.58 was found for $k_{7a}k_{8a}/k_7k_8$.

1. Introduction

It is well known that a detailed knowledge and a clear understanding of the thermal and photochemical behaviour of ozone is of fundamental importance to chemistry and aeronomy. The mechanisms of the thermal decomposition [1, 2] of ozone and of its photolysis at 600 nm [3 - 5] and 334 nm [6, 7] are well established. The situation at 253.7 nm is rather different [8, 9]. Although the fundamental mechanism at this wavelength can be considered to be established some problems still remain. The numerical values of some of the rate constants should be modified and some revised reactions should be included in the mechanism.

Several papers dealing with the reaction of $\text{O}(^1\text{D})$ atoms with O_3 [10 - 15], the fate of O_2^* molecules [14], the efficiency of production of $\text{O}_2(^1\Sigma_g^+)$ molecules [16] and their reaction with O_3 [17, 18], and the nature and efficiency of the primary process in the Hartley band [19 - 24] have been published recently. Values between 5.5 and 6 molecules quantum⁻¹ have been reported [8, 9, 14 - 25] for the quantum yield of ozone decomposition at 253.7 nm.

The purpose of this paper is to propose answers to the questions which still exist with respect to ozone photolysis at 253.7 nm and to establish a mechanism which provides a quantitative representation of all the experimental results.

2. Experimental details

Ozone is very sensitive to the presence of impurities which frequently have a catalytic effect and promote uncontrollable thermal reactions, particularly at high concentrations and elevated pressures. The photochemical decomposition of ozone in the spectral regions where excited species are formed is even more sensitive. Great care must therefore be taken to ensure the cleanliness of all parts of the apparatus coming into contact with ozone and the presence of even traces of water vapour in the system must be avoided.

The apparatus, which has been described elsewhere [26], was similar to that used with excellent results in earlier investigations. No thermal or catalytic reactions were observed in any of the experiments. A cylindrical quartz reaction cell 3 cm long with an outside diameter of 5.7 cm and parallel optically flat windows was used. A high intensity Bausch and Lomb monochromator, adjusted to a bandwidth of 10 nm, was used to isolate the 253.7 nm mercury line.

Two series of experiments were carried out. One was performed with initial ozone pressures of approximately 50 Torr and the other with initial ozone pressures of about 1 Torr. In the first series an Osram HBO high pressure mercury lamp was used as the light source and the reaction was monitored manometrically at constant temperature and volume. The pressure change was measured using a Bodenstein quartz spiral manometer as a null instrument supplemented by a mercury manometer. Most of the experiments were monitored up to a conversion of 30%.

The light intensity was measured during each irradiation period using a polished stainless steel slotted disc rotating at 78 rev min^{-1} which was located at an angle of 45° to the light beam in such a way that when the beam impinged on the slot the light passed through the reaction cell and when the beam impinged on the mirror the reflected light was directed onto a potassium ferrioxalate actinometer [27]. The system was calibrated by placing a similar actinometer in front of the reaction cell and measuring the ratio of the light intensities of the direct and the reflected beams.

The manometric method was unsatisfactory at low ozone pressures since it was not possible to determine the ozone consumption accurately without achieving appreciable conversion of O_3 to O_2 . In addition it was impossible to achieve high p_X/p_{O_3} ratios ($X \equiv$ added gas). Therefore in the second series of experiments, which were carried out at low ozone pressures (1 - 2 Torr), the ozone concentration was monitored photometrically by optical absorption at 253.7 nm. The apparatus shown schematically in Fig. 1, which is basically a double-beam photometer, was used for this purpose. A Hanovia SH,HP-100 medium pressure mercury lamp was used as the light source for photolysis and for the optical absorbance measurements. In order to ensure that negligible ozone decomposition took place during the concentration measurement the light beam intensity was attenuated using a

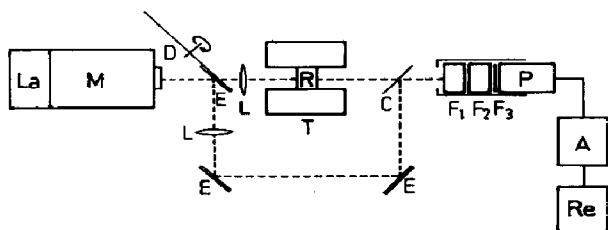


Fig. 1. Schematic diagram of the photometer: La, mercury lamp; M, monochromator; D, chopper; E, mirrors; C, quartz plate; R, reaction cell; T, thermostat; F_1 , F_2 , F_3 , filters; P, phototube; A, amplifier; Re, recorder.

detachable Schott and Gen WG 7 glass filter 2 mm thick located at the monochromator exit. The filter was removed during photolysis. A chopper consisting of a slotted disc 15 cm in diameter which rotated at 2 rev min^{-1} and was composed of a dark sector and a metallized sector which acted as a mirror split the attenuated light into a sample and a reference beam. During each third of a revolution the light beam alternately passed through the reactor cell or was reflected by the sector mirror and by means of mirrors and lenses was finally focused onto an RCA 1P28 phototube. The phototube was protected from stray light by a filter system consisting of a Schott and Gen UG 5 glass filter 2 mm thick followed by an $\text{NiSO}_4\text{-CoSO}_4$ aqueous solution of path length 5 cm [26] and a 4.2 atm chlorine gas filter also of path length 5 cm. When the light beam impinged on the darkened sector of the disc no signal was transmitted to the phototube. The optical signals received by the phototube were converted into electrical signals and transmitted via an amplifier circuit to a recorder. Thus one of the recorder signals was proportional to the energy transmitted by the sample and the other was proportional to the energy emitted by the source. The zero drift of the photometer was recorded during the period when there was no signal and was found to be negligible because the measurement of the O_3 concentration only took a few minutes in each case. Calibration of the whole system was achieved by recording the relative intensity of both beams when the reaction cell was evacuated and when it was filled with known pressures of an $\text{O}_3\text{-N}_2$ mixture. The ozone absorption calculated from its pressure and the extinction coefficient [28] was in close agreement with the photometric data.

The preparation and purification of ozone, oxygen, helium and nitrogen have been described elsewhere [26]. SF_6 supplied by the Matheson Co., U.S.A., was purified by low temperature sublimation and stored as a gas in a Pyrex flask.

3. Experiments and results

3.1. Pure ozone

Figure 2 shows the quantum yield Φ determined using the manometric method as a function of the mean oxygen pressure \bar{p}_{O_2} . These experiments were performed at a mean ozone pressure of approximately 48 Torr and a mean oxygen pressure varying between 2 and 30 Torr. In this range the quantum yield was found to be a linear function of the oxygen pressure. This makes it possible to calculate the intercept $\Phi(p_{\text{O}_2} = 0)$ for $\bar{p}_{\text{O}_2} = 0$ by linear extrapolation. A least-squares treatment gives $\Phi(p_{\text{O}_2} = 0) = 5.66 \pm 0.08$ molecules quantum $^{-1}$.

Figure 3 shows Φ determined using the photometric method *versus* \bar{p}_{O_2} . These experiments were performed at a mean ozone pressure of approximately 1 Torr and a mean oxygen pressure varying between 0.1 and 2 Torr.

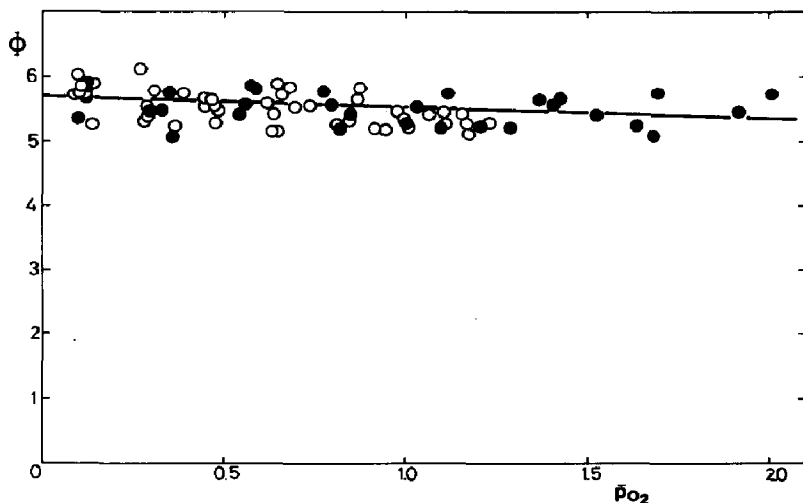


Fig. 2. Plot of the quantum yield Φ of O_3 decomposition vs. \bar{p}_{O_2} for the experiments using the manometric method ($(p_{O_3})_i = 50$ Torr).

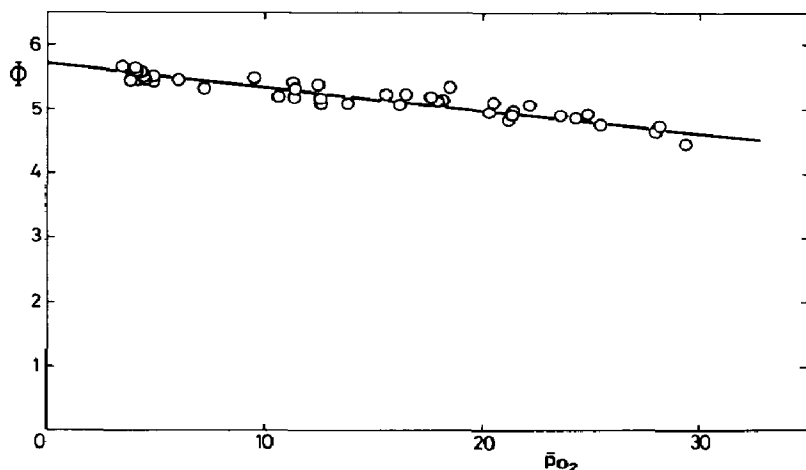


Fig. 3. Plot of the quantum yield Φ of O_3 decomposition vs. \bar{p}_{O_2} for the experiments using the photometric method: \circ , $\bar{p}_{O_3} = 1$ Torr; \bullet , $(p_{O_3})_i = 2.3$ Torr.

The observed dependence of Φ on \bar{p}_{O_2} over this range enables the intercept to be calculated by linear extrapolation. A least-squares analysis gives $\Phi(p_{O_2} = 0) = 5.70 \pm 0.13$ molecules quantum⁻¹ in close agreement with the value obtained using the manometric method. The results obtained using both methods are summarized in Table 1.

The mean value of the quantum yield Φ in oxygen-free systems is 5.68 ± 0.15 molecules quantum⁻¹. Φ is independent of ozone pressure in agreement with the results of earlier work [8, 9].

TABLE 1

Quantum yield $\Phi(p_{O_2} = 0)$ of ozone decomposition in oxygen-free systems

<i>Manometric method</i>		<i>Photometric method</i>	
p_{O_3} (Torr)	$\Phi(p_{O_2} = 0)$	p_{O_3} (Torr)	$\Phi(p_{O_2} = 0)$
50.7	5.71	2.34	5.66
50.1	5.72	1.98	5.77
49.9	5.50	2.10	5.42
51.8	5.57	2.12	5.66
50.0	5.82	1.09	5.85
50.0	5.53	1.14	5.81
50.6	5.78	1.08	5.78
50.9	5.65	1.07	5.41
49.6	5.56	1.02	5.60
51.8	5.66	1.07	5.78
49.9	5.63	1.07	5.92
50.1	5.78	1.16	5.74

3.2. O_3-O_2 mixture

The addition of oxygen to ozone produced a marked reduction in the quantum yield. Figure 4 shows the values of Φ obtained on addition of oxygen at pressures up to 600 Torr to ozone at a pressure of about 50 Torr. These results are compared with those calculated using eqn. (XXI) (Section 4) in Table 2. Figure 5 shows the values of Φ obtained in experiments in which oxygen at pressures up to 60 Torr was added to ozone at a pressure of about

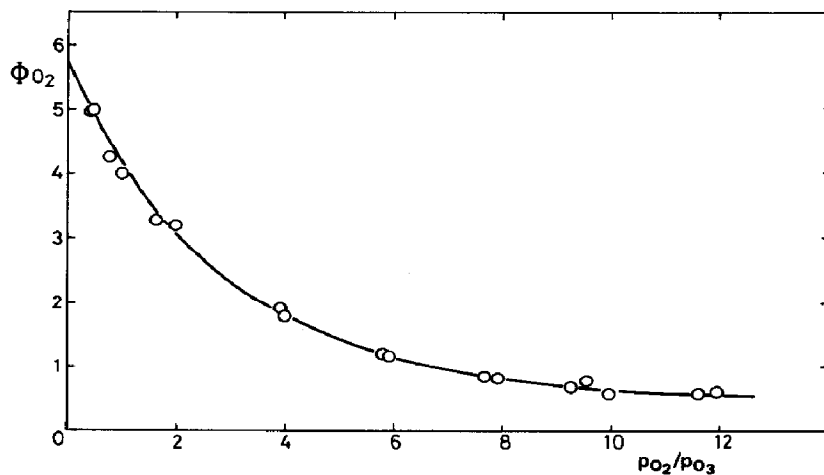


Fig. 4. Plot of the quantum yield Φ_{O_2} of O_3 decomposition vs. p_{O_2}/p_{O_3} for experiments using the manometric method ($(p_{O_3})_i = 50$ Torr): —, plotted using eqn. (XXI).

TABLE 2

Effect of the addition of oxygen on the quantum yield of ozone decomposition measured using the manometric method

p_{O_3} (Torr)	p_{O_2} (Torr)	Φ	Φ_{calc}^a
51.4	24.5	5.00	4.98
50.4	25.3	5.01	4.95
52.4	40.3	4.27	4.52
49.5	49.8	4.00	4.24
60.8	98.8	3.28	3.21
50.1	99.2	3.20	3.07
50.5	198.1	1.91	1.77
50.1	200.0	1.81	1.75
51.1	296.1	1.14	1.18
50.5	298.7	1.17	1.16
51.6	396.4	0.84	0.86
50.4	398.0	0.80	0.85
51.9	494.7	0.76	0.68
49.9	495.3	0.67	0.66
50.7	502.8	0.58	0.66
50.2	589.7	0.60	0.55
51.5	597.6	0.51	0.55

^aCalculated using eqn. (XXI) (Section 4).

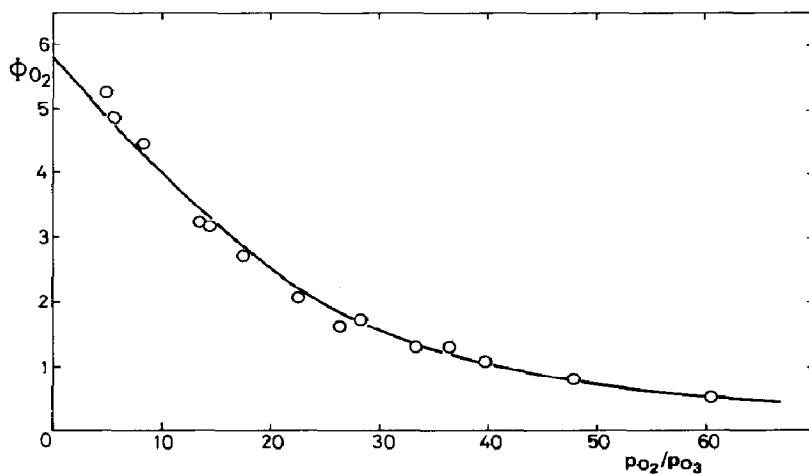


Fig. 5. Plot of the quantum yield Φ of O_3 decomposition vs. p_{O_2}/p_{O_3} for experiments using the photometric method ($(p_{O_3})_i = 1$ Torr): —, plotted using eqn. (XXI).

1 Torr. These results are compared with the values calculated using eqn. (XXI) in Table 3.

3.3. O_3 -He mixture

The effect of the addition of helium was studied using the photometric method only since it allows high p_{He}/p_{O_3} ratios to be attained. The experi-

TABLE 3

Effect of the addition of oxygen on the quantum yield of ozone decomposition measured using the photometric method

p_{O_3} (Torr)	p_{O_2} (Torr)	Φ	Φ_{calc}^a
1.11	5.5	5.24	4.95
1.09	6.2	4.87	4.84
1.09	9.1	4.45	4.35
1.11	14.9	3.23	3.42
1.10	15.9	3.22	3.26
1.15	20.2	2.68	2.73
1.15	26.1	2.07	2.10
1.11	29.4	1.62	1.79
1.06	30.1	1.73	1.69
1.03	34.5	1.31	1.38
1.10	40.1	1.13	1.17
1.12	44.6	1.06	1.01
1.07	51.2	0.75	0.79
1.03	62.5	0.51	0.55

^aCalculated using eqn. (XXI).

ments were performed by adding helium at a pressure of approximately 600 Torr to ozone at 1 - 2 Torr. Figure 6 shows the dependence of the quantum yield Φ_{He} in the presence of helium on the p_{O_2}/p_{O_3} ratio. When p_{O_2}/p_{O_3} is 0.4 or less the quantum yield is a linear function of p_{O_2}/p_{O_3} . A value of $\Phi_{\text{He}}(p_{O_2} = 0) = 5.5 \pm 0.2$ molecules quantum⁻¹, which is close to that obtained in pure ozone, is obtained from the intercept. Some experiments were also carried out in mixtures containing ozone at a pressure of 1 Torr and helium at a pressure of 700 Torr to which oxygen was added in

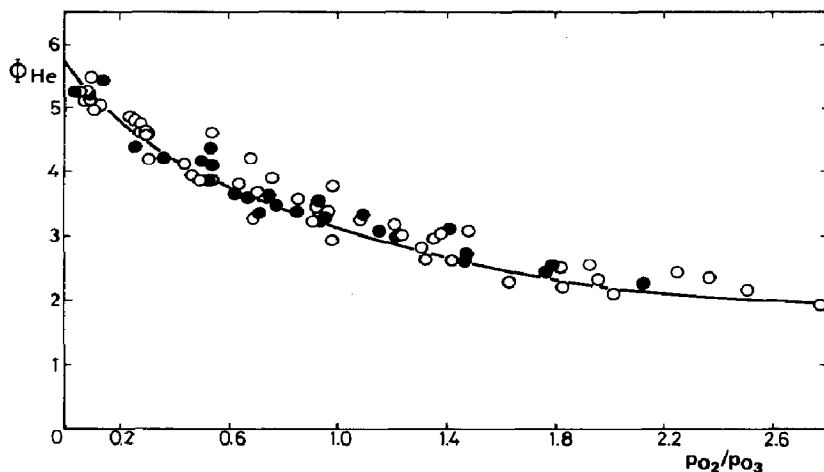


Fig. 6. Plot of the quantum yield Φ_{He} of O_3 decomposition in the presence of helium vs. p_{O_2}/p_{O_3} ($p_{\text{He}} = 600$ Torr): ○, $(p_{O_3})_i = 1$ Torr; ●, $(p_{O_3})_i = 2.3$ Torr; —, plotted using eqn. (XXI).

TABLE 4

Effect of the addition of oxygen and helium on the quantum yield $\Phi_{\text{He},\text{O}_2}$ of ozone decomposition

p_{O_3} (Torr)	p_{O_2} (Torr)	p_{He} (Torr)	$\Phi_{\text{He},\text{O}_2}$	Φ_{calc}^a
1.18	3.6	705.2	1.66	1.55
1.15	3.6	702.3	1.50	1.53
1.14	4.0	702.8	1.61	1.43
1.18	4.0	703.2	1.52	1.46
1.17	4.3	702.3	1.37	1.38
1.12	4.3	706.1	1.59	1.34
1.19	5.1	701.9	1.45	1.25
1.14	5.2	702.3	1.23	1.20
1.07	6.5	695.4	1.18	1.00
0.98	5.5	703.3	1.05	0.98

^aCalculated using eqn. (XXI).

amounts at pressures varying between 3 and 6 Torr. The results are shown in Table 4 and are compared with those calculated using eqn. (XXI).

3.4. O_3 - SF_6 mixture

Figure 7 shows the values of the quantum yield Φ_{SF_6} in the presence of SF_6 as a function of the $p_{\text{O}_2}/p_{\text{O}_3}$ ratio obtained using the photometric method. SF_6 at about 300 Torr was added to ozone at about 1 Torr. The significant non-linear dependence of Φ_{SF_6} on $p_{\text{O}_2}/p_{\text{O}_3}$ makes it difficult to obtain a reliable value of $\Phi_{\text{SF}_6}(p_{\text{O}_2} = 0)$. However, it can be seen that it is close to the value obtained in pure ozone.

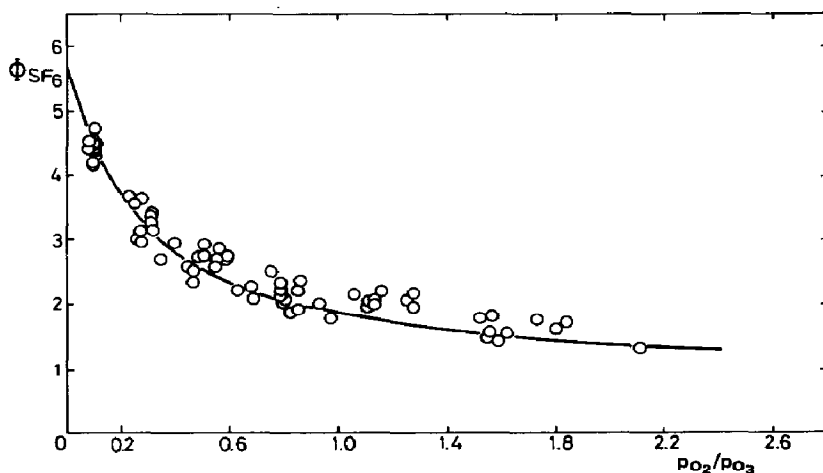


Fig. 7. Plot of the quantum yield Φ_{SF_6} of O_3 decomposition in the presence of SF_6 vs. $p_{\text{O}_2}/p_{\text{O}_3}$ ($(p_{\text{O}_3})_i = 1$ Torr; $p_{\text{SF}_6} = 300$ Torr): —, plotted using eqn. (XXI).

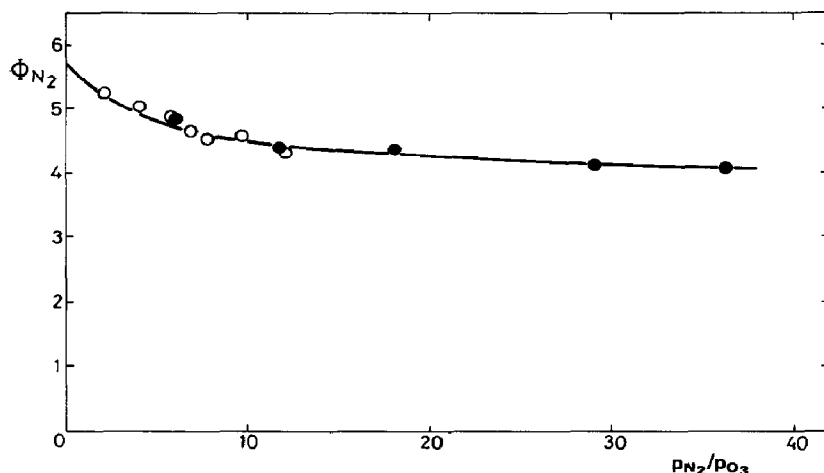


Fig. 8. Plot of the quantum yield $\Phi_{N_2}(p_{O_2} = 0)$ of O_3 decomposition in the presence of nitrogen vs. p_{N_2}/p_{O_3} : \circ , $(p_{O_3})_i = 50$ Torr; \bullet , $(p_{O_3})_i = 1$ Torr; —, plotted using eqn. (XXI).

3.5. O_3 - N_2 mixture

The effect of nitrogen was studied using both the manometric method (ozone at a pressure of 50 Torr and nitrogen at pressures up to 600 Torr) and the photometric method (ozone at a pressure of 1 Torr and nitrogen at pressures up to 40 Torr). Plots of the quantum yield as a function of p_{O_2}/p_{O_3} for each experiment showed that for $p_{O_2}/p_{O_3} \leq 0.7$ the quantum yield Φ_{N_2} in the presence of nitrogen is a linear function of p_{O_2}/p_{O_3} . The

TABLE 5

Effect of the addition of nitrogen on the quantum yield $\Phi_{N_2}(p_{O_2} = 0)$ of ozone decomposition

p_{O_3} (Torr)	p_{N_2} (Torr)	$\Phi_{N_2}(p_{O_2} = 0)$	$\gamma_{N_2}^a$
48.0	101.8	5.23	0.17
49.9	201.1	5.03	0.15
51.6	297.8	4.86	0.15
1.03	6.2	4.83	0.15
49.8	347.5	4.63	0.20
50.7	396.9	4.54	0.22
51.3	499.2	4.57	0.17
0.97	11.4	4.37	0.23
49.7	600.9	4.32	0.25
1.02	18.5	4.41	0.13
1.03	30.1	4.12	0.21
1.12	40.8	4.03	0.27

^aThe efficiency of deactivation of $O(^1D)$ by nitrogen calculated using eqn. (XXI).

value of $\Phi_{N_2}(p_{O_2} = 0)$ for each nitrogen pressure was obtained from the intercept. Figure 8 shows a plot of $\Phi_{N_2}(p_{O_2} = 0)$ versus p_{N_2}/p_{O_3} . It can be seen that the limiting quantum yield at large p_{N_2}/p_{O_3} ratios approaches 4 molecules quantum⁻¹. Table 5 gives the values of $\Phi_{N_2}(p_{O_2} = 0)$ for various nitrogen pressures together with the efficiency of deactivation of O(¹D) atoms by nitrogen calculated using eqn. (XXI). The mean value obtained is $\gamma_{N_2} = 0.19 \pm 0.01$.

Tables 6 - 14 show the results of some typical experiments carried out under various conditions. In these tables $(p_{O_3})_i$ and $(p_{O_2})_i$ are the initial

TABLE 6
Experiment 120

Δp (Torr)	\bar{p}_{O_3} (Torr)	\bar{p}_{O_2} (Torr)	$J \times 10^{-18}$ (quanta)	Φ	Φ_{calc}
2.5	48.1	4.1	2.21	5.61	5.59
2.3	43.3	11.3	2.09	5.46	5.37
2.3	38.7	18.2	2.23	5.12	5.14

$(p_{O_3})_i = 50.6$ Torr; $(p_{O_2})_i = 0.3$ Torr; $\Phi(p_{O_2} = 0) = 5.78$ molecules quanta⁻¹.

TABLE 7
Experiment 96

Δp (Torr)	\bar{p}_{O_3} (Torr)	\bar{p}_{O_2} (Torr)	$J \times 10^{-18}$ (quanta)	Φ	Φ_{calc}
1.3	49.1	400.0	8.24	0.78	0.83
1.3	46.5	403.9	8.31	0.78	0.79
1.3	43.9	407.8	8.82	0.73	0.75

$(p_{O_3})_i = 50.4$ Torr; $(p_{O_2})_i = 398.0$ Torr.

TABLE 8
Experiment 159

Δp (Torr)	\bar{p}_{O_3} (Torr)	\bar{p}_{O_2} (Torr)	$J \times 10^{-18}$ (quanta)	Φ	Φ_{calc}
3.1	47.6	4.9	3.74	4.11	4.14
2.8	41.7	13.8	3.85	3.61	3.40
2.2	36.7	21.3	3.77	2.89	2.84
1.9	32.6	27.4	3.88	2.43	2.43

$(p_{O_3})_i = 50.7$ Torr; $(p_{O_2})_i = 0.3$ Torr; $p_{N_2} = 396.9$ Torr; $\Phi_{N_2}(p_{O_2} = 0) = 4.54$ molecules quanta⁻¹.

TABLE 9

Experiment 32

Δt (min)	Δp_{O_3} (Torr)	\bar{p}_{O_3} (Torr)	\bar{p}_{O_2} (Torr)	$J' \times 10^{-16}$ (quanta)	Φ	Φ_{calc}
11	0.144	1.91	0.12	6.158	5.80	5.70
11	0.136	1.77	0.33	6.213	5.43	5.68
13	0.169	1.62	0.56	7.216	5.81	5.66
14	0.163	1.45	0.80	7.266	5.56	5.63
15	0.164	1.29	1.04	7.323	5.55	5.59
17	0.158	1.13	1.29	7.575	5.17	5.55
18	0.161	0.97	1.53	7.380	5.41	5.50

$(p_{O_3})_i = 1.98$ Torr; $(p_{O_2})_i = 0.01$ Torr; $\Phi(p_{O_2} = 0) = 5.77$ molecules quanta⁻¹.

TABLE 10

Experiment 111

Δt (min)	Δp_{O_3} (Torr)	\bar{p}_{O_3} (Torr)	\bar{p}_{O_2} (Torr)	$J' \times 10^{-17}$ (quanta)	Φ	Φ_{calc}
76	0.100	1.02	51.28	3.433	0.72	0.76
91	0.100	0.92	51.43	3.818	0.65	0.69
100	0.096	0.82	51.57	4.079	0.58	0.62
105	0.092	0.73	51.71	4.272	0.53	0.55

$(p_{O_3})_i = 1.07$ Torr; $(p_{O_2})_i = 51.2$ Torr.

TABLE 11

Experiment 68

Δt (min)	Δp_{O_3} (Torr)	\bar{p}_{O_3} (Torr)	\bar{p}_{O_2} (Torr)	$J' \times 10^{-16}$ (quanta)	Φ	Φ_{calc}
18	0.118	1.04	0.10	5.380	5.44	5.23
21	0.106	0.93	0.27	5.782	4.55	4.48
26	0.104	0.82	0.43	6.773	3.81	3.85
32	0.110	0.72	0.60	8.047	3.39	3.27
39	0.106	0.61	0.76	8.683	3.03	2.75
53	0.096	0.50	0.91	10.31	2.31	2.27

$(p_{O_3})_i = 1.10$ Torr; $(p_{O_2})_i = 0.01$ Torr; $p_{\text{He}} = 601.0$ Torr.

ozone and oxygen pressures, p_{He} , p_{SF_6} , and p_{N_2} are the pressures of the added gases, \bar{p}_{O_3} and \bar{p}_{O_2} are the mean pressures in each irradiation period, Δp is the increase in total pressure after the absorption of J quanta, Δp_{O_3} is the reduction in the ozone concentration produced in Δt min by the absorption

TABLE 12

Experiment 119

Δt (min)	Δp_{O_3} (Torr)	\bar{p}_{O_3} (Torr)	\bar{p}_{O_2} (Torr)	$J' \times 10^{-17}$ (quanta)	Φ	Φ_{calc}
40	0.109	1.12	4.38	1.966	1.37	1.33
45	0.101	1.01	4.54	2.120	1.18	1.22
60	0.104	0.91	4.69	2.540	1.02	1.11
65	0.104	0.81	4.85	2.762	0.94	1.00
65	0.098	0.71	5.01	2.662	0.91	0.89

$(p_{O_3})_i = 1.17$ Torr; $(p_{O_2})_i = 4.3$ Torr; $p_{He} = 702.3$ Torr.

TABLE 13

Experiment 167

Δt (min)	Δp_{O_3} (Torr)	\bar{p}_{O_3} (Torr)	\bar{p}_{O_2} (Torr)	$J' \times 10^{-16}$ (quanta)	Φ	Φ_{calc}
14	0.135	1.05	0.11	7.660	4.37	4.36
18	0.111	0.93	0.30	8.769	3.14	3.09
22	0.098	0.82	0.46	9.533	2.55	2.45
27	0.085	0.73	0.60	10.72	1.97	2.02
33	0.098	0.64	0.74	12.15	2.00	1.68
41	0.081	0.55	0.87	14.37	1.40	1.42

$(p_{O_3})_i = 1.11$ Torr; $(p_{O_2})_i = 0.01$ Torr; $p_{SF_6} = 302.3$ Torr.

TABLE 14

Experiment 73

Δt (min)	Δp_{O_3} (Torr)	\bar{p}_{O_3} (Torr)	\bar{p}_{O_2} (Torr)	$J' \times 10^{-16}$ (quanta)	Φ	Φ_{calc}
21	0.106	0.98	0.09	5.562	4.73	4.70
32	0.142	0.85	0.28	7.601	4.63	4.62
45	0.171	0.70	0.51	9.488	4.47	4.50
67	0.186	0.52	0.78	11.16	4.13	4.35
80	0.157	0.34	1.04	9.698	4.01	4.12

$(p_{O_3})_i = 1.03$ Torr; $(p_{O_2})_i = 0.01$ Torr; $p_{N_2} = 6.2$ Torr; $\Phi_{N_2}(p_{O_2} = 0) = 4.83$ molecules quanta⁻¹.

of J' quanta and Φ and Φ_{calc} are respectively the experimental quantum yield of ozone decomposition and the value calculated using eqn. (XXI).

4. Discussion

In an attempt to establish a reaction mechanism able to explain quantitatively all the experimental data we analysed the following set of elementary reactions:



O_2^* and O_3^* are energetic molecules that can dissociate O_3 . The type of excitation is not well understood but this does not affect the following treatment. In our experimental conditions $p_{\text{M}} = p_{\text{N}_2}$ because neither helium nor SF_6 deactivate $\text{O}({}^1\text{D})$ atoms appreciably [29, 30]. M' is any stable molecule acting as a third body in the recombination process [10]. M'' and M''' are any gases present in the system with the exception of ozone.

Reactions (1a), (2a), (3), (4a) and (6) - (10) have been proposed in earlier mechanisms [8, 9] and reactions (2b), (2c), (4b), (5a) and (5b) have been proposed recently by a number of different workers.

Reaction (1b) was introduced by Fairchild *et al.* [19] in order to explain the results of their photofragment spectroscopy studies. They concluded that at 274 nm about 10% of the products of reaction (1) are formed in their ground electronic state. The same results were reported at 266 nm by Sparks *et al.* [20]. Brock and Watson [21] investigated the photolysis of ozone by a resonance fluorescence technique and found a quantum yield of 0.12 ± 0.02 atoms quantum⁻¹ for the production of ground state oxygen atoms. Finally, Amimoto *et al.* [22] measured the production of oxygen atoms at 248 nm by atomic absorption spectroscopy and found a quantum yield of 0.15 ± 0.02 atoms quantum⁻¹ for reaction (1b).

Reaction (2b) was proposed by Bair and coworkers [10, 11] who studied the UV photolysis of ozone at low pressures. Giachardi and Wayne

[12] investigated the photolysis of ozone at 254 nm in a flow system by measuring the production of oxygen atoms by resonance fluorescence and concluded that reaction (2b) occurs in approximately one-third of the reactive collisions between $O(^1D)$ and O_3 . Arnold and Comes [14] have recently investigated the photolysis of ozone at 266 nm. Their results are consistent with the occurrence of reactions (2a) and (2b) to the same extent.

Reaction (2c) was suggested by Amimoto *et al.* [13]. They found that one oxygen atom is produced for each deactivated $O(^1D)$ atom in the photolysis of ozone at 248 nm. If O_3^* is produced in reaction (2c) it must be an energetic molecule and its fate could be to decompose O_3 as in reaction (5a) or to be deactivated as in reaction (5b).

When a steady state is assumed for the reactive intermediates the proposed set of reactions leads to the following expression for the quantum yield Φ of ozone decomposition:

$$\Phi = - \frac{1}{J_{\text{abs}}} \frac{dp_{O_3}}{dt}$$

$$= 2\phi\alpha_a\theta_2 + 2\rho(1 + \phi[\theta_2\{\alpha_a\beta + 2\alpha_b + \alpha_c(1 + \eta) - 1\} + 1 + \tau\delta(1 - \theta_2 - \theta_6)])$$
(I)

where ϕ is the quantum yield of the ozone decomposition in the primary process (1a) and

$$\alpha_a = \frac{1}{1 + k_{2b}/k_{2a} + k_{2c}/k_{2a}}$$
(II)

$$\alpha_b = \frac{1}{1 + k_{2a}/k_{2b} + k_{2c}/k_{2b}}$$
(III)

$$\alpha_c = \frac{1}{1 + k_{2a}/k_{2c} + k_{2b}/k_{2c}}$$
(IV)

$$\theta_2 = \frac{1}{1 + (k_6/k_2)(p_M/p_{O_3}) + (k_7/k_2)(p_{O_2}/p_{O_3})}$$
(V)

where

$$k_2 = k_{2a} + k_{2b} + k_{2c}$$

$$k_7 = k_{7a} + k_{7b}$$

$$p_M = p_{N_2}$$

$$\theta_6 = \frac{1}{1 + (k_2/k_6)(p_{O_3}/p_M) + (k_7/k_6)(p_{O_2}/p_M)}$$
(VI)

$$\beta = \frac{1}{1 + (k_{4b}/k_{4a})(p_{M''}/p_{O_3})}$$
(VII)

$$p_{M''} = p_{O_2} + \sum_X \gamma_X'' p_X \quad (\text{VIII})$$

where p_X is p_{N_2} , p_{He} or p_{SF_6} , and the γ_X'' are their respective efficiencies in reaction (4b);

$$\eta = \frac{1}{1 + (k_{5b}/k_{5a})(p_{M''}/p_{O_2})} \quad (\text{IX})$$

$$p_{M'''} = p_{O_2} + \sum_Y \gamma_Y''' p_Y \quad (\text{X})$$

where p_Y is p_{N_2} , p_{He} or p_{SF_6} , and the γ_Y''' are their respective efficiencies in reaction (5b);

$$\tau = \frac{1}{1 + k_{7b}/k_{7a}} \quad (\text{XI})$$

$$\delta = \frac{1}{1 + k_{8b}/k_{8a}} \quad (\text{XII})$$

$$\rho = \frac{1}{1 + (k_{10}/k_9)(p_{O_2} p_{M'}/p_{O_3})} \quad (\text{XIII})$$

$$p_{M'} = p_{O_3} + \sum_Z \gamma_Z' p_Z \quad (\text{XIV})$$

where p_Z is p_{N_2} , p_{He} or p_{SF_6} , and the γ_Z are their respective efficiencies ($\gamma_{O_3}' = 1$) in recombination process (10).

In pure ozone $p_{O_2} = 0$, $p_M = p_{M''} = 0$, $p_{M'} = p_{O_3}$ and eqn. (I) reduces to

$$\Phi_{O_2=0} = 4\phi + 2 \quad (\text{XV})$$

It can be deduced from our experimental value of $\Phi = 5.68 \pm 0.15$ that the quantum yield ϕ for the primary process is 0.92 ± 0.04 molecules quantum⁻¹. This value would be somewhat smaller if the vibrationally excited oxygen molecules produced in reaction (1b) were able to dissociate O_3 or if, as suggested by Washida *et al.* [31], $O_2(^1\Delta_g)$ were formed in reaction (9). However, it is concluded from the results of the thermal [1, 2] and the photochemical decomposition of O_3 at 600 and 334 nm [5 - 7] that these contributions, if they exist, must be very small.

In the experiments carried out in the presence of added oxygen the p_{O_2}/p_{O_3} ratio was varied over a wide range. This made it possible to perform a numerical analysis of eqn. (I).

When eqn. (I) is rearranged we obtain for $p_M = 0$

$$\Phi = 2\phi\alpha_a\theta_2 + 2\{1 + \phi(1 + \tau\delta)\}\rho + 2\phi\{\alpha_a\beta + 2\alpha_b + \alpha_c(1 + \eta) - 1 - \tau\delta\}\rho\theta_2$$

which by substituting

$$A = 2\phi\alpha_a \quad (\text{XVI})$$

$$B = 2\{1 + \phi(1 + \tau\delta)\} \quad (\text{XVII})$$

$$C = 2\phi\{\alpha_a\beta + 2\alpha_b + \alpha_c(1 + \eta) - 1 - \tau\delta\} \quad (\text{XVIII})$$

can be rewritten

$$\Phi = A\theta_2 + B\rho + C\rho\theta_2 \quad (\text{XIX})$$

in which A and B are true constants. Since the efficiencies of reactions (4b) and (5b) must be low compared with those of (4a) and (5a) respectively, *i.e.* $\beta \approx \eta \approx 1$, C can also be considered as a constant. A least-squares treatment of the data using $k_7/k_2 = 0.15$ [29, 32], $k_{10}/k_9 = 5.5 \times 10^{-3} \text{ Torr}^{-1}$ [5] and $\gamma_{\text{O}_2}' = 0.44$ [5] gives $A = 0.86$, $B = 4.93$ and $C = -0.09$. When these values are substituted in eqn. (XIX) an overall quantum efficiency for pure ozone of $5.70 \text{ molecules quantum}^{-1}$ is obtained, in good agreement with the experimental result.

The product of the efficiencies of reactions (7a) and (8a) is given by eqn. (XVII) from which a value of 0.58 is calculated for $\tau\delta$. This is in good agreement with the value of 0.61 ± 0.06 recently reported by Amimoto and Wiesenfeld [18] and rather larger than the value of 0.48 ± 0.04 reported by Slinger and Black [17]. If $\tau = 0.80$ [29] is assumed for the efficiency of reaction (8a) a value of 0.73 is obtained for δ .

Equation (XIX) can be rearranged as follows:

$$\frac{\Phi}{2\theta_2} = \frac{A}{2} + \frac{B + C\theta_2}{2} \frac{\rho}{\theta_2} \quad (\text{XX})$$

Figure 9 shows that a plot of $\Phi_{\text{O}_2}/2\theta_2$ versus ρ/θ_2 yields a linear relationship over the whole range studied. The intercept $A/2$ and the slope $(B + C\theta_2)/2$ are calculated by a least-squares treatment to be 0.44 ± 0.14 and 2.41 ± 0.11 respectively. In order to account for the observed linearity $C\theta_2$ must be much less than B and consequently $B/2 \approx 2.41 \pm 0.11$. The overall quantum yield in pure ozone determined from these data is $5.70 \pm 0.25 \text{ molecules quantum}^{-1}$.

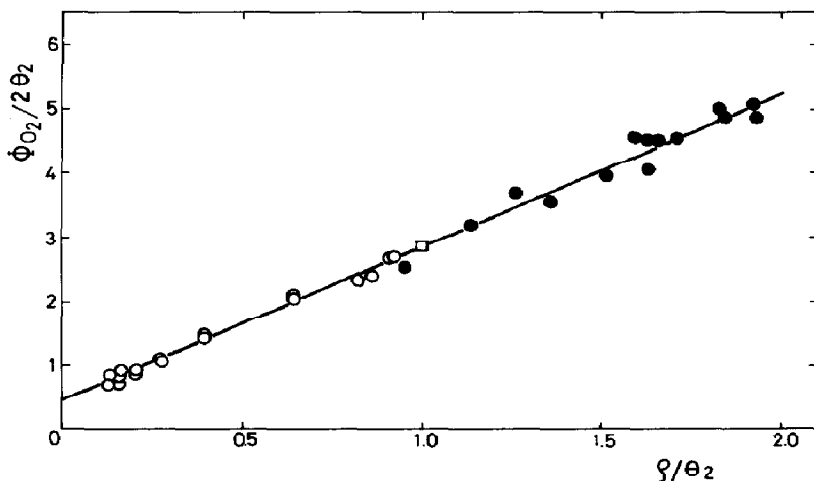


Fig. 9. Plot of $\Phi_{\text{O}_2}/2\theta_2$ vs. ρ/θ_2 for the experiments performed in the presence of oxygen: \circ , $(p_{\text{O}_3})_i = 50 \text{ Torr}$; \bullet , $(p_{\text{O}_3})_i = 1 \text{ Torr}$; \square , pure ozone.

The efficiency α_a of reaction (2a) can be calculated from eqn. (XVI) with $\phi = 0.92 \pm 0.04$ and is found to be 0.47 ± 0.15 . It is not possible to determine from our experiments whether reaction (2a) is accompanied by (2b) or (2c) or both. However, consideration of all the experimental data discussed above suggests that reaction (2c), if it exists, is unimportant compared with reactions (2a) and (2b). Therefore we have assumed that 47% of reaction (2) occurs via (2a) and 53% occurs via (2b).

The quantum yield $\Phi_{\text{He}}(p_{\text{O}_2} = 0)$ determined in the experiments performed in the presence of helium is 5.50 ± 0.20 molecules quantum⁻¹ which is close to the value of 5.68 ± 0.15 obtained in pure ozone. These results confirm that helium is an inefficient quencher of $\text{O}(^1\text{D})$ atoms and of $\text{O}_2(^1\Delta_g)$ and O_2^* molecules [33, 34]. Figure 10 shows that a plot of $\Phi_{\text{He}}/2\theta_2$ versus ρ/θ_2 in which the data points were obtained by assuming a value of 0.34 [5] for the efficiency γ_{He} of He as the third body in reaction (10) yields a linear relationship over the whole range studied. The intercept $A/2$ and the slope $B/2 \approx (B + C\theta_2)/2$ were calculated by a least-squares treatment to be 0.57 ± 0.16 and 2.24 ± 0.24 respectively. When these data are substituted in eqn. (XIX) a value of 5.62 ± 0.41 molecules quantum⁻¹ is obtained for $\Phi_{\text{He}}(p_{\text{O}_2} = 0)$.

Valuable information concerning reaction (2) can be obtained from the experiments carried out in the presence of helium and oxygen. It can be seen that reaction (2a) followed by (4a) produces one oxygen atom whereas reaction (2b) produces two. In oxygen-free systems both processes lead to the same value for the overall quantum yield. However, in the presence of significant amounts of oxygen some of the oxygen atoms re-form ozone via reaction (10) and therefore the overall quantum yield depends on the relative importance of reactions (2a) and (2b). The overall quantum yield for $\text{O}_3\text{-O}_2\text{-He}$ mixtures was calculated using eqn. (XXI) with $\alpha_a = 0.47$ and $\alpha_b =$

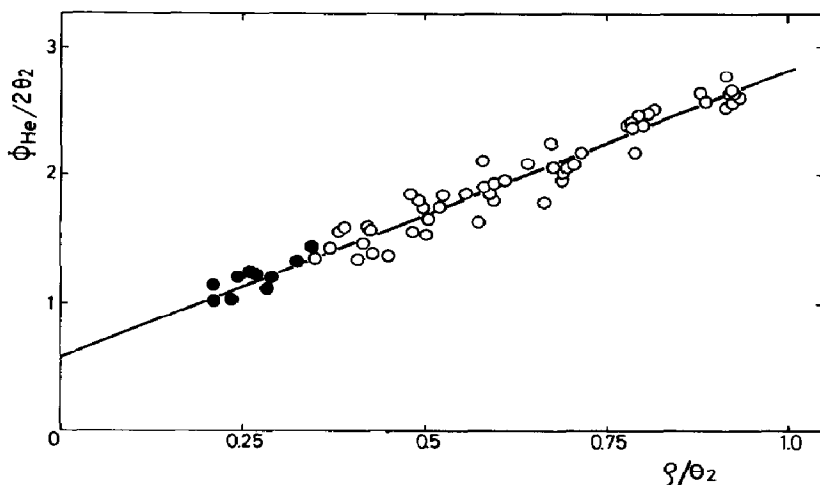


Fig. 10. Plot of $\Phi_{\text{He}}/2\theta_2$ vs. ρ/θ_2 for experiments performed in the presence of helium: \circ , $(p_{\text{O}_3})_i = 1$ Torr; $p_{\text{He}} = 600$ Torr; \bullet , $(p_{\text{O}_3})_i = 1$ Torr, $(p_{\text{O}_2})_i = 3 - 6$ Torr, $p_{\text{He}} = 600$ Torr.

0.53. The results (Table 4) are in close agreement with the experimental data.

The addition of SF_6 to pure ozone produces only a small change in the quantum yield as does the addition of helium. However, in the presence of significant amounts of oxygen the quantum yield is reduced much more by SF_6 than by helium (Fig. 7). The line in Fig. 7 was drawn using eqn. (XXI) and assuming a value of 2.17 [35] for the efficiency γ_{SF_6}' of SF_6 in reaction (10). This value is in good agreement with $\gamma_{\text{SF}_6}' = 2.12$ calculated using the values $34 \times 10^{-34} \text{ cm}^6 \text{ molecule}^{-2} \text{ s}^{-1}$ [36] or $31 \times 10^{-34} \text{ cm}^6 \text{ molecule}^{-2} \text{ s}^{-1}$ [37] or $22.5 \times 10^{-34} \text{ cm}^6 \text{ molecule}^{-2} \text{ s}^{-1}$ [38] for $k_{10}(M' \equiv \text{SF}_6)$, $k_{10}(M' \equiv \text{O}_2) = 6.07 \times 10^{-34} \text{ cm}^6 \text{ molecule}^{-1} \text{ s}^{-1}$ [39] and $\gamma_{\text{O}_2}' = 0.44$ [5].

A plot of $\Phi_{\text{SF}_6}/2\theta_2$ versus ρ/θ_2 yields a linear relationship over the range studied (Fig. 11). The intercept $A/2$ and the slope $(B + C\theta_2)/2$ were calculated by a least-squares treatment to be 0.63 ± 0.08 and 2.09 ± 0.21 respectively. In order to account for the observed linearity $C\theta_2$ must be much less than B and consequently $B/2 \approx 2.09 \pm 0.21$. These data give a value for the overall quantum yield $\Phi_{\text{SF}_6}(p_{\text{O}_2} = 0)$ of a mixture consisting of SF_6 at 300 Torr and ozone at 1 Torr of 5.44 ± 0.32 molecules quantum $^{-1}$ which is slightly lower than the value of 5.68 ± 0.15 molecules quantum $^{-1}$ found for pure ozone. This small effect, if it exists, must be ascribed to the deactivation of active intermediates. It is well known that neither $\text{O}(^1\text{D})$ nor $\text{O}_2(^1\Delta_g)$ are effectively deactivated by SF_6 [29, 30]. If it is assumed that O_2^* is the only excited molecule quenched by SF_6 , the efficiency of SF_6 as a deactivator in reaction (4b) can be estimated to be $\gamma_{\text{SF}_6}'' = k_{4b}(M'' \equiv \text{SF}_6)/k_{4a} \approx 7 \times 10^{-4}$. Therefore it can be concluded that O_2^* is highly resistant to collisional deactivation and consequently $\beta \approx 1$.

When all the preceding considerations ($\alpha_c = 0$, $\beta = 1$, $\eta = 1$) are taken into account, eqn. (I) simplifies to

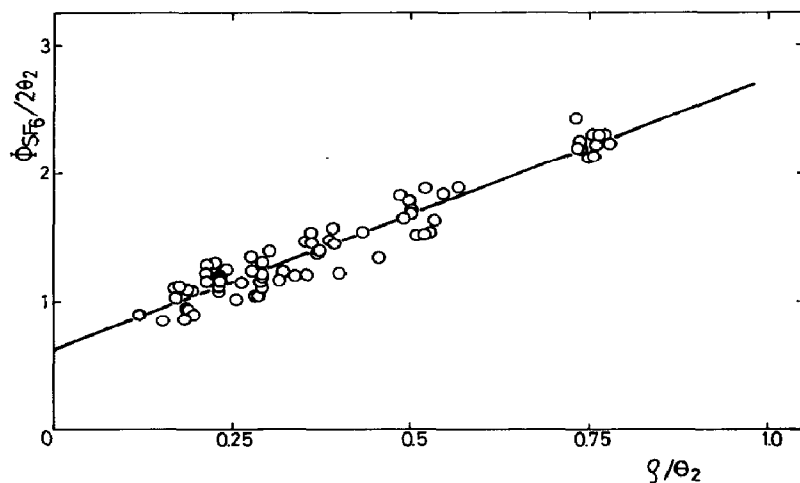


Fig. 11. Plot of $\Phi_{\text{SF}_6}/2\theta_2$ vs. ρ/θ_2 for the experiments performed in the presence of SF_6 : $(p_{\text{O}_2})_i = 1 \text{ Torr}$; $p_{\text{SF}_6} = 300 \text{ Torr}$.

$$\Phi = 2\phi\alpha_a\theta_2 + 2\rho[1 + \phi\{\theta_2(1 - \alpha_a) + 1 + \tau\delta(1 - \theta_2 - \theta_6)\}] \quad (\text{XXI})$$

When eqn. (XXI) is applied to oxygen-free $\text{O}_3\text{-N}_2$ systems with $p_{\text{N}_2}/p_{\text{O}_3} \rightarrow \infty$, $\Phi = 2(1 + \phi)$. When $\phi = 0.92$ is substituted a value of 3.84 molecules quantum⁻¹ is obtained for $\Phi(p_{\text{N}_2}/p_{\text{O}_3} \rightarrow \infty)$, in good agreement with the experimental value obtained at high nitrogen pressures (Fig. 8). When eqn. (XXI) is used with a value of 0.39 [5] for the efficiency γ_{N_2}' of N_2 as a third body in reaction (10) the efficiency of nitrogen as a quencher for $\text{O}(^1\text{D})$ atoms in reaction (6) is $\gamma_{\text{N}_2} = 0.19 \pm 0.01$ (Table 5), in close agreement with the values obtained in previous work [8, 9] and that recommended by Baulch *et al.* [39].

5. Conclusion

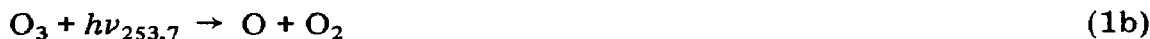
The reactions



and therefore



can be ignored under our experimental conditions. The experimental data can therefore be explained using the following mechanism:



The overall quantum yield for the decomposition of pure ozone is $\Phi = 5.68 \pm 0.15$ molecules quantum⁻¹ and is pressure independent. The

addition of helium up to a ratio $p_{\text{He}}/p_{\text{O}_2} \approx 600$ has no effect on Φ in oxygen-free systems and the addition of SF_6 up to a ratio $p_{\text{SF}_6}/p_{\text{O}_2} \approx 300$ has only a small effect on Φ . When nitrogen is added at high $p_{\text{N}_2}/p_{\text{O}_2}$ ratios, Φ_{N_2} tends towards 4 molecules quantum⁻¹.

Oxygen has a strong inhibitory effect. The quantum yield ϕ for $\text{O}(^1\text{D})$ production is 0.92 ± 0.04 atoms quantum⁻¹. The efficiency of deactivation of $\text{O}(^1\text{D})$ atoms by nitrogen is $\gamma_{\text{N}_2} = 0.19 \pm 0.01$. $\text{O}(^1\text{D})$ reacts with O_3 via (2a) producing the unspecified energetic O_2^* molecule with an efficiency of 47% and via (2b) producing two oxygen atoms with an efficiency of 53%. O_2^* is very resistant to collisional deactivation.

The product $\tau\delta = k_{7a}k_{8a}/k_7k_8$ of the branching ratios of reactions (7a) and (8a) is 0.58. Thus if τ is taken as 0.80 [29], the efficiency δ of reaction (8a) is 0.73.

When the values $k_7/k_2 = 0.15$ [29, 32], $k_{10}/k_9 = 5.5 \times 10^{-3}$ [5], $\gamma_{\text{O}_2}' = 0.44$ [5], $\gamma_{\text{N}_2}' = 0.39$ [5], $\gamma_{\text{He}}' = 0.34$ [5] and $\gamma_{\text{SF}_6}' = 2.17$ [35] are assumed, the quantum yield for ozone decomposition calculated using eqn. (XXI) is in very good agreement with experiment.

Acknowledgment

C. Cobos is a Fellow of the Consejo Nacional de Investigaciones Científicas y Técnicas, Argentina.

References

- 1 A. Glissman and H. J. Schumacher, *Z. Phys. Chem., Abt. B*, **21** (1933) 323.
- 2 S. W. Benson and A. E. Axworthy, *J. Chem. Phys.*, **26** (1957) 1718.
- 3 G. B. Kistiakowsky, *Z. Phys. Chem., Abt. B*, **117** (1925) 337.
- 4 H. J. Schumacher, *J. Am. Chem. Soc.*, **52** (1930) 2377.
- 5 E. Castellano and H. J. Schumacher, *Z. Phys. Chem. N.F.*, **34** (1962) 198.
- 6 E. Castellano and H. J. Schumacher, *Chem. Phys. Lett.*, **13** (1972) 625.
- 7 E. Castellano and H. J. Schumacher, *Z. Phys. Chem. N.F.*, **83** (1973) 54.
- 8 G. von Ellenrieder, E. Castellano and H. J. Schumacher, *Chem. Phys. Lett.*, **9** (1971) 152.
- 9 G. von Ellenrieder, E. Castellano and H. J. Schumacher, *Z. Phys. Chem. N.F.*, **76** (1971) 240.
- 10 H. Webster III and E. J. Bair, *J. Chem. Phys.*, **53** (1971) 4532.
- 11 V. D. Baiamonte, L. G. Hartshorn and E. J. Bair, *J. Chem. Phys.*, **55** (1971) 3617.
- 12 D. J. Giachardi and R. P. Wayne, *Proc. R. Soc. London, Ser. A*, **330** (1972) 131.
- 13 S. T. Amimoto, A. P. Force and J. R. Wiesenfeld, *Chem. Phys. Lett.*, **60** (1978) 40.
- 14 I. Arnold and F. J. Comes, *Chem. Phys.*, **47** (1980) 125.
- 15 P. H. Wine and A. R. Ravishankava, *Chem. Phys. Lett.*, **77** (1981) 103.
- 16 L. C. Lee and T. G. Slanger, *J. Chem. Phys.*, **69** (1978) 4051.
- 17 T. G. Slanger and G. Black, *J. Chem. Phys.*, **70** (1979) 3434.
- 18 S. T. Amimoto and J. R. Wiesenfeld, *J. Chem. Phys.*, **72** (1980) 3899.
- 19 C. E. Fairchild, E. J. Stone and G. M. Lawrence, *J. Chem. Phys.*, **69** (1978) 3632.
- 20 R. K. Sparks, L. R. Carlson, K. Shobatake, M. L. Kowalczyk and Y. T. Lee, *J. Chem. Phys.*, **72** (1980) 1401.

- 21 J. C. Brock and R. T. Watson, *Chem. Phys. Lett.*, **71** (1980) 371.
- 22 S. T. Amimoto, A. P. Force, J. R. Wiesenfeld and R. H. Young, *J. Chem. Phys.*, **73** (1980) 1244.
- 23 O. Kajimoto and R. J. Cvetanovic, *Int. J. Chem. Kinet.*, **11** (1979) 605.
- 24 P. W. Fairchild and E. K. C. Lee, *Chem. Phys. Lett.*, **60** (1978) 36.
- 25 E. Lissi and J. Heicklen, *J. Photochem.*, **1** (1972) 39.
- 26 E. Castellano and H. J. Schumacher, *Z. Phys. Chem. N.F.*, **65** (1969) 62.
- 27 C. G. Hatchard and C. A. Parker, *Proc. R. Soc. London, Ser. A*, **235** (1956) 518.
- 28 M. Griggs, *J. Chem. Phys.*, **49** (1968) 857.
- 29 D. L. Baulch, R. A. Cox, R. F. Hampson, J. A. Kerr, J. Troe and R. T. Watson, *J. Phys. Chem. Ref. Data*, **9** (1980) 295.
- 30 W. M. Jones and N. Davidson, *J. Am. Chem. Soc.*, **84** (1962) 2868.
- 31 N. Washida, H. Akimoto and M. Okuda, *Bull. Chem. Soc. Jpn.*, **53** (1980) 3496.
- 32 R. D. Hudson and E. I. Reed (eds.), *The Stratosphere: Present and Future, NASA Ref. Publ. 1049*, December 1979 (Goddard Space Flight Center, National Aeronautics and Space Administration).
- 33 K. Schofield, *J. Photochem.*, **9** (1978) 55.
- 34 F. D. Findlay and D. R. Snelling, *J. Chem. Phys.*, **55** (1971) 545.
- 35 H. S. Johnson, *Gas Phase Reaction Kinetics of Neutral Oxygen Species, NBS Natl. Stand. Ref. Data Ser. 20*, 1968 (National Bureau of Standards, U.S. Department of Commerce).
- 36 F. Kaufman and J. R. Kelso, *J. Chem. Phys.*, **46** (1967) 4541.
- 37 P. L. T. Bevan and G. R. Johnson, *J. Chem. Soc., Faraday Trans. I*, **69** (1973) 216.
- 38 H. Endo, K. Glänzer and J. Troe, *J. Phys. Chem.*, **83** (1979) 2083.
- 39 D. L. Baulch, D. D. Drysdale, J. Duxbury and S. J. Grant, *Evaluated Kinetic Data for High Temperature Reactions*, Vol. 3, Butterworths, London, 1976.